

Torsional_Strength.docx

by

Submission date: 12-Sep-2018 01:15PM (UTC+0700)

Submission ID: 1000566356

File name: Torsional_Strength.docx (779.75K)

Word count: 3224

Character count: 16205

Torsional Strength Prediction of RC Hybrid Deep T-Beam with an Opening using Softened Truss Model

Lisantono, A.¹, Besari, M. S.², and Suhud, R.²

Introduction

In order to pass utility (ducts and pipes) and also to save headroom, an opening is often required in the beam. Beam with opening subjected to pure torsion is very rare. Normally it is subjected to combination of bending, shear and torsion. However, it is important to study the beam under pure torsion as the basis of understanding their complex behavior under combine loadings [1]. Researches in torsion of shallow beam were extensively carried out [2-8], however, research in torsion of deep beams is rare and attracts little attention. Beams with span/depth ratios about four or less are categorized as deep beams [9]. Akhtaruzzaman and Hasnat [10] conducted investigation on the torsional behavior of deep beams with and without opening, while Samman et al [11] reported their investigations on the torsional behavior of rectangular plain concrete deep beams without opening.

Lisantono et al. [12] has reported preliminary investigation on the effect of light weight concrete (LWC) flanges and web opening on the torsional capacity of RC deep T-beams. Lisantono et al. [13,14] also investigate the effect of web opening locations,

11

¹ Department of Civil Engineering, Universitas Atma Jaya Yogyakarta, Yogyakarta, INDONESIA.

Email: adelisantono@mail.uajy.ac.id

² Department of Civil Engineering, Institut Teknologi Bandung, Bandung, INDONESIA

Note: Discussion is expected before June, 1st 2013, and will be published in the "Civil Engineering Dimension" volume 15, number 2, September 2013.

Received 17 November 2011; revised 26 July 2012; accepted 15 February 2013

in horizontal as well as in vertical direction, on the torsional behavior of RC deep T-beam. To obtain a clear understanding on the effect of web opening dimension on the torsional behavior of RC hybrid deep T-beams, Lisantono et al [15] conducted an experimental program. This study aims to develop a method for predicting the torsional capacity of RC hybrid deep T-beam, especially deep T-beam with web opening.

Softened Truss Model Theory

A beam subjected to pure torsion will behave as an analogous thin wall tube-space truss [2-6]. After the beam cracks, concrete strut will be subjected to compression force and the reinforcement acts as a tie. Hsu [16] stated that three equilibrium conditions Truss Model satisfy Mohr's stress circle and by assuming that the steel bars can only resist axial stresses, superposition of concrete stresses gives:

$$\sigma_l = \sigma_d \cos^2 \alpha + \sigma_r \sin^2 \alpha + \rho f_t \quad (1)$$

$$\sigma_t = \sigma_d \sin^2 \alpha + \sigma_r \cos^2 \alpha + \rho f_t \quad (2)$$

$$\tau_{lt} = (-\sigma_d + \sigma_r) \sin \alpha \cos \alpha \quad (3)$$

where

σ_l, σ_t = normal stresses in the direction of longitudinal steel bar (the l direction) and the direction of transverse steel bar (the t direction), respectively (positive for tension)

τ_{lt} = shear stresses in the l-t coordinate (positive as shown in Figure 1)

σ_d, σ_r = principal stresses in the d and r directions, respectively (positive for tension)

α = angle of inclination of the d-axis with respect to l axis

ρ_b, ρ_t = reinforcement ratios in the l and t directions

as $\frac{A_l}{p_o t_d}$ and $\frac{A_t}{s t_d}$

f_l, f_t = steel stresses in the l and t - directions, respectively

A_l, A_t = area of total longitudinal steel bars and area of one leg of stirrup, respectively.

p_o = periphery of shear flow center line

s = stirrups spacing

According to the Bredt's theory which stated that shear flow should be constant along the centerline of the shear flow zone and can be related to the torque, T. Hsu [4] adding one more equilibrium equation:

$$T = \tau_{lt} (2A_o t_d) \quad (4)$$

where

T = torque

A_o = the area within the centerline of the shear flow

t_d = the effective thickness of shear flow

Hsu [16] showed that from the compatibility condition of the truss model, the average strains satisfy the Mohr's strain circle and gives the following equations:

$$\epsilon_l = \epsilon_d \cos^2 \alpha + \epsilon_r \sin^2 \alpha \quad (5)$$

$$\epsilon_t = \epsilon_d \sin^2 \alpha + \epsilon_r \cos^2 \alpha \quad (6)$$

$$\gamma_{lt} = 2(-\epsilon_d + \epsilon_r) \sin \alpha \cos \alpha \quad (7)$$

where

ϵ_l, ϵ_t = average strain in the l and t directions, respectively (positive for tension)

γ_{lt} = average shear strains in the l-t coordinate (positive as shown in Figure 1)

ϵ_d, ϵ_r = average principal strains in the d and r directions, respectively (positive for tension)

The stress and strain of concrete in the d direction

follows material law proposed by Vecchio and Collin [17] for the softened concrete:

$$\sigma_d = \zeta f_c' \left[\frac{2 \left(\frac{\epsilon_d}{\zeta \epsilon_0} \right) - \left(\frac{\epsilon_d}{\zeta \epsilon_0} \right)^2}{\left(\frac{\epsilon_d}{\zeta \epsilon_0} \right) + \left(\frac{\epsilon_d}{\zeta \epsilon_0} \right)} \right] \text{ for } |\epsilon_d| \leq |\zeta \epsilon_0| \quad (8.a)$$

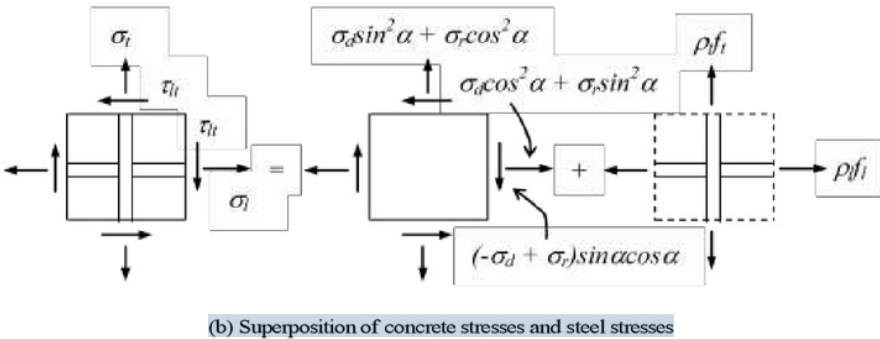
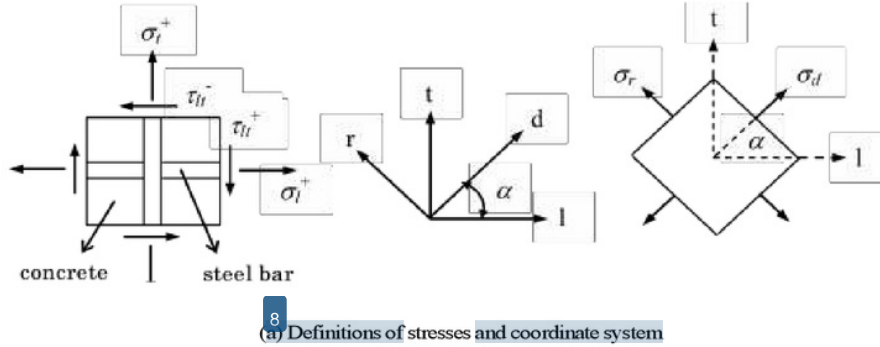


Figure 1. Stress Condition in Reinforced Concrete Element [16]

$$\sigma_d = \zeta f_c \left[1 - \left(\frac{\epsilon_d - \zeta}{\epsilon_o - \zeta} \right)^2 \right] \text{ for } \left| \frac{\epsilon_d - \zeta}{\epsilon_o - \zeta} \right| \leq 1 \quad (8.b)$$

with

$$\zeta = \sqrt{\frac{\epsilon_d}{(1-\mu)\epsilon_d - \epsilon_r}} \quad (9.a)$$

where

σ_d = compression stress at the concrete strut

ζ = softening coefficient

μ = Poisson ratio

ϵ_o = strain at the maximum compressive stress of nonsoftened concrete and can be taken as 0.002 [4].

Hsu [7] used the softening coefficient as proposed by Belarbi and Hsu [18] as follows:

$$\zeta = \frac{0.9}{1 + 600\epsilon_r} \quad (9.b)$$

The stress-strain relationship in the r direction can be expressed by

$$\sigma_r = E_c \epsilon_r \text{ for } \epsilon_r \leq \epsilon_{cr} \quad (10.a)$$

$$\sigma_r = \frac{f_{cr}}{1 + \sqrt{\frac{\epsilon_r - \epsilon_{cr}}{0.005}}} \text{ for } \epsilon_r > \epsilon_{cr} \quad (10.b)$$

where

E_c = modulus of elasticity of concrete

ϵ_{cr} = strain at cracking of concrete, taken to be $\frac{f_{cr}}{E_c}$

f_{cr} = stress at torsional cracking of concrete is assumed to occur when the principal tensile stress reaches the tensile strength of the concrete in biaxial tension-compression and can be taken as $\frac{1}{3} \sqrt{f_c}$ [19]

The stress-strain relationship for longitudinal and transverse steel bars are assumed to be elastic-perfectly plastic.

Softened Truss Model for RC Hybrid Deep T-beam

According to CEB-FIP Model Code 1990 [20] for beam consisting of several rectangular sections, the torque of the beam can be assumed to be distributed on each rectangular section as:

$$T_i = T \frac{X_i^3 Y_i}{\sum_{ii} X_i^3 Y_i} \quad (11)$$

where

T = total torque

T_i = torque that assumed to be resisted by the- i^{th} section

X_i = the smaller size of the- i^{th} section

Y_i = the larger size of the- i^{th} section

The RC hybrid deep T-beam in this research was cast of normal weight concrete web and light weight concrete flanges as shown in the Figure 2.a.

If the flange portion and web portion are denoted as I and II, respectively, the proportion of each torque becomes:

$$T_I = T \frac{h_f^3 b_f}{(b_w^3 h_w + h_f^3 b_f)} \quad (12)$$

$$T_{II} = T \frac{b_w^3 h_w}{(b_w^3 h_w + h_f^3 b_f)} \quad (13)$$

Considering the web opening in the beam (Figure 2.b), Equation 12 and 13 become:

$$T_I = T \frac{h_f^3 b_f}{\left\{ \frac{b_w^3 (h_w - d_o)}{3} + h_f^3 b_f \right\}} \quad (14)$$

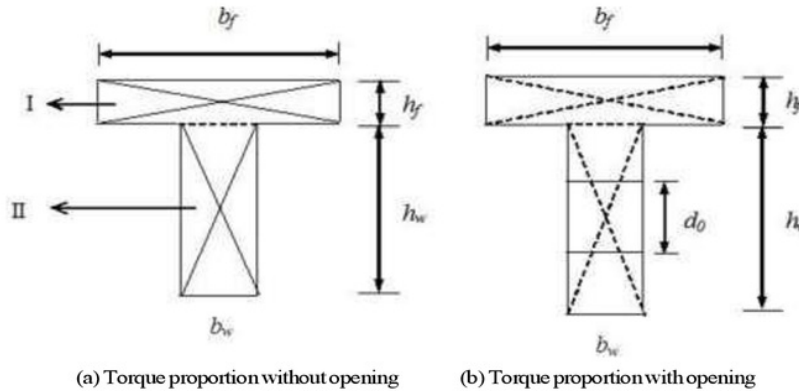


Figure 2. Torque Proportion of the RC Hybrid Deep T-beam

$$T_{II} = T \left\{ \frac{b_w^3 (h_w - d_o)^3}{b_w h_w - d_o} + \frac{b_f^3}{h} \right\} \quad (15)$$

where

T = total torque

T_I = torque resisted by flange (light weight concrete)

T_{II} = torque resisted by web (normal weight concrete)

b_f = width of flange

h_f = thickness of flange

b_w = width of web

h_w = height of web

d_o = opening diameter

To derive the torque capacity of a RC hybrid deep T-beam after cracking the beam is assumed to be a space truss-thin wall tube analog as shown in Figure 3. Figure 3 shows that the shear flow of flange section (light weight concrete) is q_I and the effective thickness of shear flow zone is t_{dI} , while the shear flow and the effective thickness of web section (normal weight concrete) are q_{II} and t_{dII} , respectively. Taking a small element A at flange section and B at web section of the RC hybrid deep T-beam as shown in Figure 3, the shear stress of element A will be:

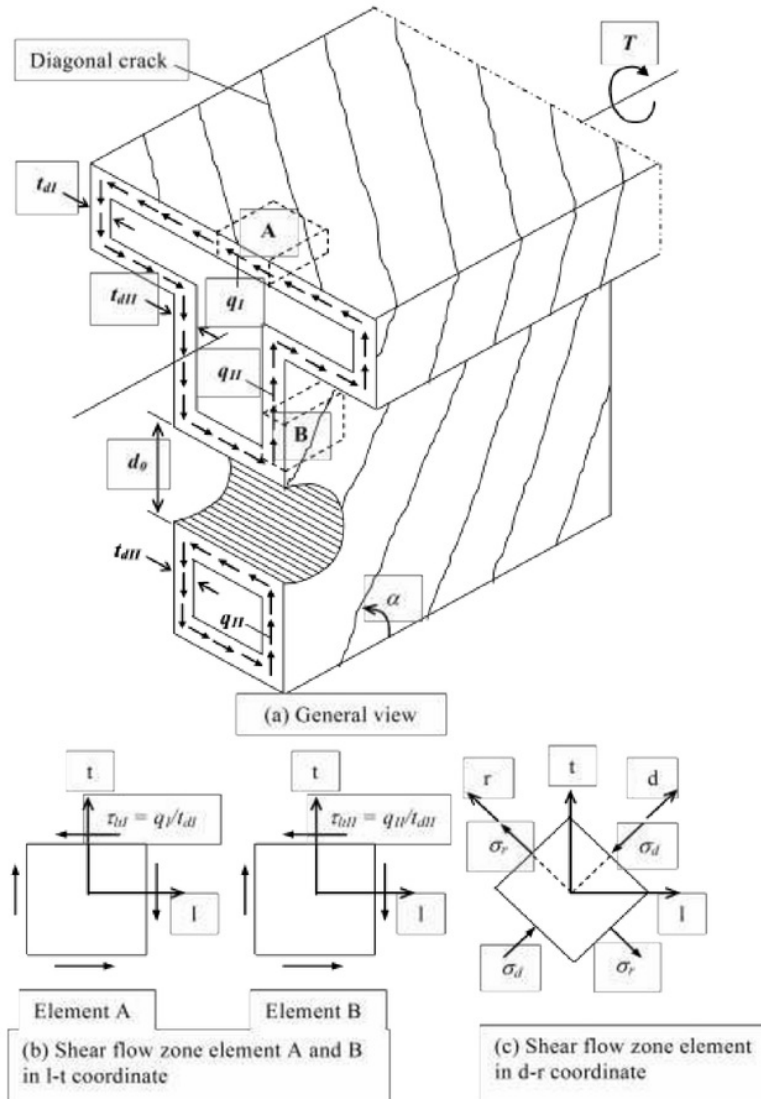


Figure 3. Space Truss-Thin Wall Tube Analogy for RC Hybrid Deep T-beam with Opening

$$\tau_{II} = \frac{q_I}{t_{dI}} \quad (16)$$

Therefore, the shear flow in the flange section is

$$q_I = \tau_{II} t_{dI} \quad (17)$$

Similarly the shear stress and shear flow of element B in web section are;

$$\tau_{III} = \frac{q_{II}}{t_{dII}} \quad (18)$$

$$q_{II} = \tau_{III} t_{dII} \quad (19)$$

According to the Bredt's theory [4] the shear flow q must be constant along the shear flow center line. Therefore, the relationship of shear flow of light weight and normal weight concrete can be obtained as:

$$q_I = q_{II} \quad (20)$$

Substituting Equations 17 and 19 into Equation 20 gives:

$$\tau_{II} t_{dI} = \tau_{III} t_{dII} \quad (21)$$

Assuming that the stress and strain of the light weight and normal weight concrete satisfy the equilibrium condition of membrane element (Equation 3), gives the relationship at the light weight and normal weight concrete as

$$\tau_{II} = (-\sigma_{dI} + \sigma_{rI}) \sin \alpha_I \cos \alpha_I \quad (22)$$

$$\tau_{III} = (-\sigma_{dII} + \sigma_{rII}) \sin \alpha_{II} \cos \alpha_{II} \quad (23)$$

Hsu [5] stated that as long as the tensile strength (σ_r) of the concrete is very small compared to the compressive strength (σ_d), the effect on the torque will be small too. Therefore, the tensile strength (σ_r) can be neglected in the analysis. Substituting $\sigma_{rI} = \sigma_{rII} = 0$ into Equations 22 and 23, gives

$$\tau_{II} = -\sigma_{dI} \sin \alpha_I \cos \alpha_I \quad (24)$$

$$\tau_{III} = -\sigma_{dII} \sin \alpha_{II} \cos \alpha_{II} \quad (25)$$

Substituting Equations 24 and 25 into Equation 21 gives

$$-\sigma_{dI} \sin \alpha_I \cos \alpha_I t_{dI} = -\sigma_{dII} \sin \alpha_{II} \cos \alpha_{II} t_{dII} \quad (26)$$

Experimental results [12-15] show that diagonal cracking angle of the light weight and normal weight zone is the same, hence:

$$\alpha_I = \alpha_{II} = \alpha \quad (27)$$

Therefore, Equation 26 can be reduced as

$$-\sigma_{dI} t_{dI} = -\sigma_{dII} t_{dII} \quad (28)$$

Equation 28 illustrates that the compressive force at the strut of light weight concrete must be in equilibrium condition with the compressive force at the strut of normal weight concrete. Therefore, if the characteristics of light weight and normal weight concrete are not the same, the effective thickness of shear flow zone or t_d must not be the same either.

Lampert and Thurlimann [21,22] proposed that due to warping, the strut concrete is not only subjected to compressive force but also flexure at the tubewall. This phenomenon can be stated in curvature equation as:

$$\psi = 2\theta \sin \alpha \cos \alpha \quad (29)$$

where,

ψ = curvature of concrete strut

According to the flexural phenomenon at the tube wall, the curvature of concrete strut at each light weight and normal weight concrete can be obtained as:

$$\psi_I = \theta_I 2 \sin \alpha_I \cos \alpha_I \quad (30)$$

$$\psi_{II} = \theta_{II} 2 \sin \alpha_{II} \cos \alpha_{II} \quad (31)$$

Due to the composite condition of the light weight and normal weight concrete, therefore the twist angle of the light weight concrete is the same as the twist angle of the normal weight concrete, hence

$$\theta_I = \theta_{II} = \theta \quad (32)$$

Considering that $\alpha_I = \alpha_{II} = \alpha$ (Equation 27) and $\theta_I = \theta_{II} = \theta$ (Equation 32), Equation 30 is the same with Equation 31, therefore giving

$$\psi_I = \psi_{II} = \psi \quad (33)$$

Equation 33 implies that the curvature at the light weight concrete strut is the same as the curvature at the normal weight concrete strut, hence the strain diagram block of light weight concrete strut in the flanges and normal weight concrete strut in the web of the beam can be plotted as shown in Figure 4.

Since $\psi_I = \psi_{II} = \psi$, it can be obtained that (see Figure 4):

$$\frac{\epsilon_{dSI}}{t_{dI}} = \frac{\epsilon_{dSI}}{t_{dII}} \quad (34)$$

If $\epsilon_{dSI} = 2\epsilon_{dI}$ and $\epsilon_{dSI} = 2\epsilon_{dII}$ (see Figure 4),

Equation 34 can be rewritten as:

$$\frac{\epsilon_{dI}}{t_{dI}} = \frac{\epsilon_{dII}}{t_{dII}} \quad (35)$$

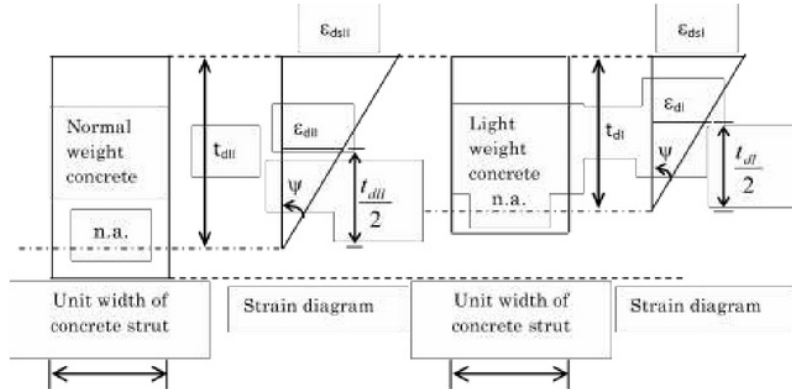


Figure 4. Curvature at the Strut of Light Weight and Normal Weight Concrete

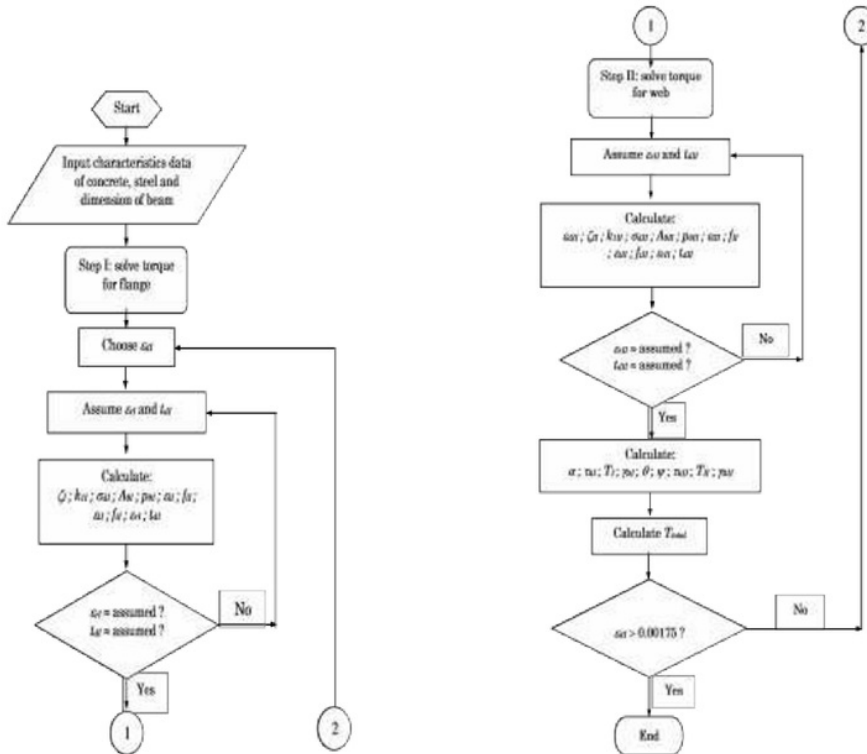


Figure 5. Flow Chart of Calculation of RC Hybrid Deep T-beam Torque

Based on Equations 27, 28, 32, 33; and Equation 35 the softened truss model for RC hybrid deep T-beam with web opening can be developed [23]. By using FORTRAN, the flow chart of calculation to predict the torque capacity of RC hybrid deep T-beam with web opening can be seen in Figure 5.

It is to be noted that program was terminated when ϵ_{dl} has reached the value of 0.00175 or $\epsilon_{dsl} = 0.0035$, where ϵ_{dsl} is the compression strain of concrete at the outer surface of diagonal concrete strut, while ϵ_{dl} is the compression strain of concrete at the middle height of the effective thickness of the diagonal concrete strut (see Figure 4).

Experimental Program

To verify the theory, Lisantonio et al [15] conducted experimental program of torsional RC hybrid deep-T beams. Four beams namely B4HS; B4HOD1; B4HO; and B4HOD3 were prepared. The first beam (B4HS) was reinforced concrete hybrid deep T-beam without opening, cast of normal weight concrete web and light weight concrete flanges.

The second, third and fourth beams (B4HOD1; B4HO and B4HOD3) were reinforced concrete hybrid deep T-beams with web opening diameters of 100 mm; 200 mm and 300 mm, respectively. The circular openings were located at mid span and mid depth of the beam. All beams have the same span of 2000 mm and the same nominal cross-sectional dimensions. Details of the beams are shown in Figures 6, 7, 8, and 9.

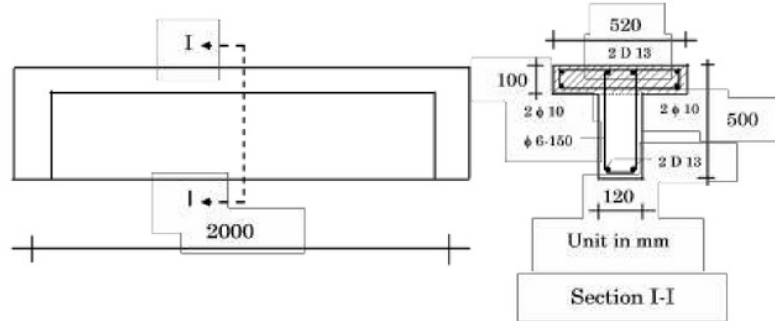


Figure 6. Specimen B4HS

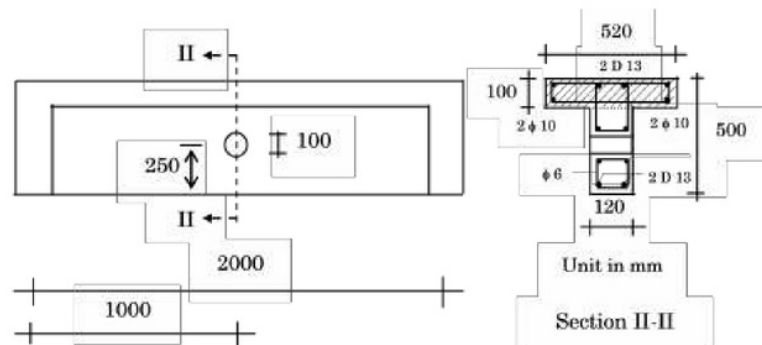


Figure 7. Specimen B4HOD

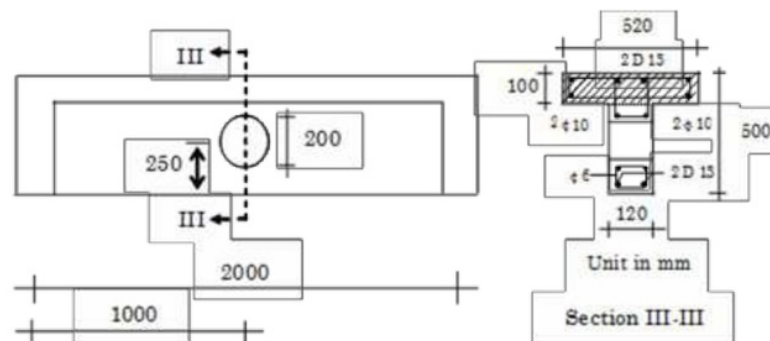


Figure 8. Specimen B4HO

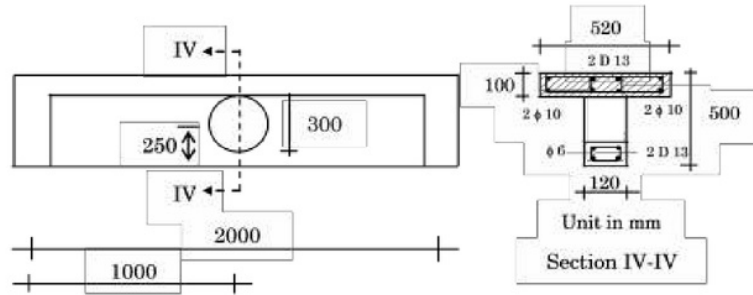


Figure 9. Specimen B4HOD3

B4HS and B4HO were cast out of batches different from those of B4HOD1 and B4HOD3. The mechanical properties of the concrete are shown in Table 1.

Table 1. The Properties of Concretes

Specimen	B4HS & B4HO		B4HOD1 & B4HOD3	
	NWC	LWC	NWC	LWC
Density (kg/m ³)	2356.96	1721.98	2374.20	1780.65
f'_c (MPa)	35.40	40.74	35.68	40.03
f_{sp} (MPa)	3.32	2.79	3.41	2.76
E_c (GPa)	25.15	14.70	26.04	15.57
μ (Poisson ratio)	0.18-0.22	0.18-0.26	0.19-0.26	0.19-0.23

The test setup of the specimen is illustrated in Figure 10. The beams were instrumented for measurements of prevailing deflections and rotations. The deflections and rotations due to the torque force were measured using LVDT and inclinometers respectively. The electrical resistance strain gauges were used to measure strains in reinforcements and concrete.

Results and Discussion

Comparison between the experimental results and the softened truss model theory of the beam B4HS, B4HOD1, B4HO, and B4HOD3 can be seen in Figures 11, 12, 13, and 14, respectively.

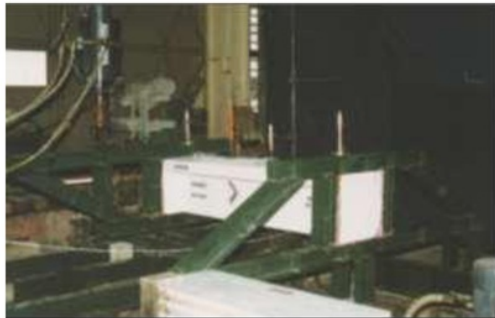


Figure 10. Test Setup of the Specimen

The experimental results show that generally the strength characteristics of the tested beams up to first cracking behave essentially linear. After first cracking, preceded by a small drop in torque, the curves increased non-linearly with increasing twist up to their ultimate torque. It was observed that the small drop in torque occurred when the crack propagated a short distance along the corner line of the web-flange interface. After reaching their ultimate torque, the curves decreased non-linearly with increasing twist, and proceeded with a section of an approximately horizontal plateau, indicating a state of yielding prior to collapse [15].

Figures 11, 12, 13, and 14, show that the theory can predict not only the torsional strength of the RC hybrid deep-T beam, but also the angle of twist throughout the post-cracking loading history. Comparing to the experimental results, it can be seen that generally the stiffness of the tested beam is stiffer than the curve predicted by the theory. To evaluate the accuracy of proposed theory, the torque capacity and twist angle predicted by the proposed theory were compared to the experimental results. Comparison of the maximum torque capacity based on the proposed theory with the experimental results can be seen in Table 2.

Table 2. Comparison of the Maximum Torque Capacity

Number	Beam	$T_{ult} (anl.)$ (kNm)	$T_{ult} (exp.)$ (kNm)	$T_{ult}(anl.) / T_{ult}(exp.)$	Differences (%)
1	B4HS	14.310	14.697	0.974	2.6
2	B4HOD1	14.293	14.246	1.003	0.3
3	B4HO	13.582	13.660	0.994	0.6
4	B4HOD3	11.850	12.317	0.962	3.8

$T_{ult} (anl.)$: maximum torque capacity based on the softened truss model

$T_{ult} (exp.)$: maximum torque capacity based on experimental program

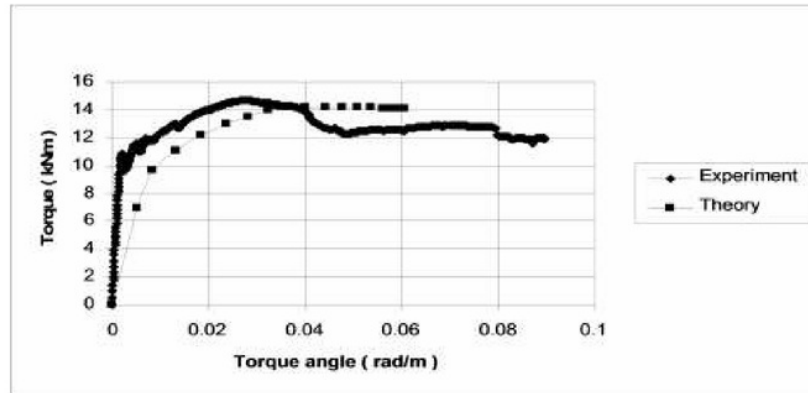


Figure 11. Comparison Result of the Beam B4HS

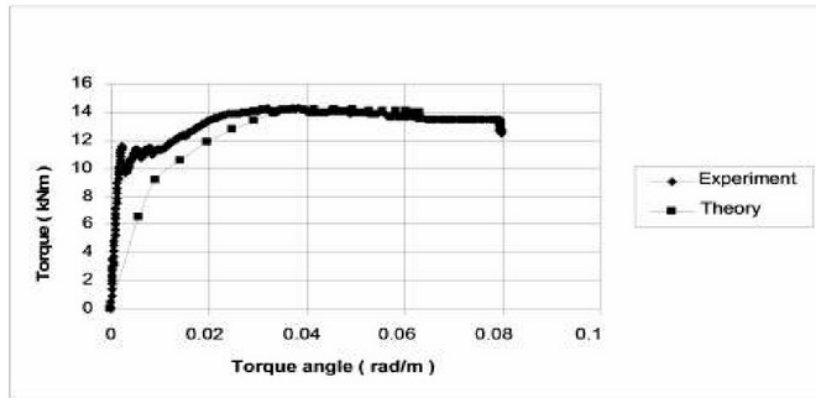


Figure 12. Comparison Result of the Beam B4HOD1

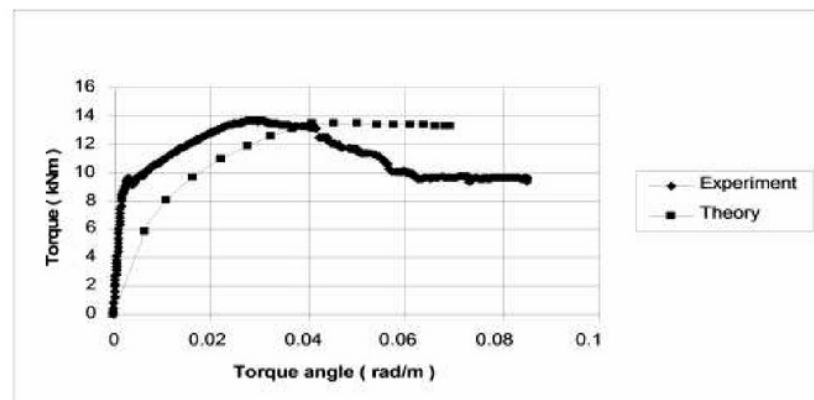


Figure 13. Comparison Result of the Beam B4HO

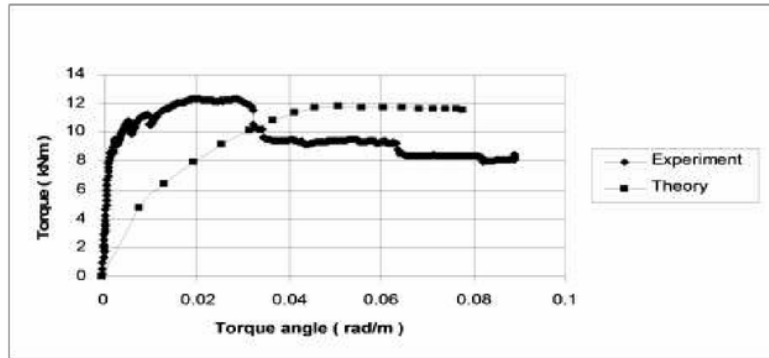


Figure 14. Comparison Result of the Beam B4HOD3

Table 2 shows that the softened truss model can accurately predict the maximum torque capacity of RC hybrid deep T-beam.

The comparison of the twist angle at maximum torque obtained using the softened truss model with the experimental results can be seen in Table 3.

Table 3. Comparison the Maximum Twist Angle

Number	Beam	$\theta_{ult}(anl.)$ ($\times 10^{-3} rad/m$)	$\theta_{ult}(exp.)$ ($\times 10^{-3} rad/m$)	$\theta_{ult}(anl.) / \theta_{ult}(exp.)$	Differences (%)
1	B4HS	38.21971	28.152	1.358	35.8
2	B4HOD1	40.38389	32.301	1.250	25.0
3	B4HO	44.14396	29.226	1.510	51.0
4	B4HOD3	50.33863	21.436	2.348	134.8

$\theta_{ult}(anl.)$: the maximum twist angle based on the softened truss model

$\theta_{ult}(exp.)$: the maximum twist angle based on the experimental program

Table 3 shows that the maximum twist angle predicted by the theory is higher than the experimental result. It means that twist angle predicted by the theory gives more excessive twist angle than the experimental results, especially for the beam with the large opening. It is suspected, this softer behavior is due to the fact that the proposed method was derived based on the assumption that the concrete of the beam was already crack, while in reality the beam has two behavior condition throughout the loading history that is before first cracking and after cracking of the concrete.

Conclusion

Based on comparison of the results between analytical method and experimental program, the following conclusions can be drawn. The softened truss model can predict not only the torsional strength of the RC hybrid deep-T beam, but also the

angle of twist throughout the post-cracking loading history.

Prediction of the maximum torque capacity of the RC hybrid deep T-beams based on the softened truss model is close to the experimental results. However, the twist angle predicted by the softened truss model is higher than to the experimental results, especially for the beam with large opening. The excessive prediction of the twist angle is due to the fact that the softened truss model was derived based on the assumption that the concrete of the beam was already crack, while in reality the beam has two behavior condition throughout the loading history, that are before first cracking and after first cracking of the concrete.

Acknowledgement

The first author would like to thank Professor Mohamad Sahari Besari, Professor Ridwan Suhud and Biemo Wuryanto Soemardi, Ph.D. for their kind assistance to the author during his study for Doctoral degree in Institut Teknologi Bandung (ITB), Indonesia. The first author also thanks the Laboratory of Structures and Materials, Civil Engineering Department of ITB, and the Laboratory of Structural Mechanics of the Inter University Research Center of ITB for the use of their research facilities.

ORIGINALITY REPORT

16%

SIMILARITY INDEX

7%

INTERNET SOURCES

12%

PUBLICATIONS

4%

STUDENT PAPERS

PRIMARY SOURCES

1

pl.scribd.com

Internet Source

3%

2

Hsu, Thomas T. C.. "Toward A Unified Nomenclature for Reinforced-Concrete Theory", Journal of Structural Engineering, 1996.

Publication

2%

3

P.G. Bakir, H.M. Boduroglu. "Nonlinear analysis of beam-column joints using softened truss model", Mechanics Research Communications, 2006

Publication

1%

4

Submitted to Universitas Diponegoro

Student Paper

1%

5

Hyunjin Ju, Deuck Hang Lee, Jin-Ha Hwang, Joo-Won Kang, Kang Su Kim, Young-Hun Oh. "Torsional behavior model of steel-fiber-reinforced concrete members modifying fixed-angle softened-truss model", Composites Part B: Engineering, 2013

1%

6	repository.petra.ac.id Internet Source	1 %
7	Kachi Mohand Said, Bouafia Youcef, Idir Abdelkader. "Simulation of the Influence of the Confinement, Until Fracture, on the Shear Stiffness of the Reinforced or Prestressed Concrete", Procedia Materials Science, 2014 Publication	1 %
8	"Advances in Structural Engineering", Springer Nature America, Inc, 2015 Publication	1 %
9	Ahmed E. Salama, Magdy E. Kassem, Ahmed A. Mahmoud. "Torsional behavior of T- shaped reinforced concrete beams with large web openings", Journal of Building Engineering, 2018 Publication	1 %
10	Bakir, P.G.. "Mechanical behaviour and non-linear analysis of short beams using softened truss and direct strut & tie models", Engineering Structures, 200503 Publication	1 %
11	Submitted to Universitas Atma Jaya Yogyakarta Student Paper	1 %

- | | | |
|----|--|------|
| 12 | Lee, Jung-Yoon, Sang-Woo Kim, and Mohamad Y. Mansour. "Nonlinear Analysis of Shear-Critical Reinforced Concrete Beams Using Fixed Angle Theory", Journal of Structural Engineering, 2011.
Publication | <1 % |
| 13 | Wen-Yao Lu. "Shear strength of high-strength concrete dapped-end beams", Journal of the Chinese Institute of Engineers, 07/2003
Publication | <1 % |
| 14 | Royset, Johannes O., Armen Der Kiureghian, and Elijah Polak. "Optimal Design with Probabilistic Objective and Constraints", Journal of Engineering Mechanics, 2006.
Publication | <1 % |
| 15 | Submitted to Cork Institute of Technology
Student Paper | <1 % |
| 16 | Ade Lisantono, Haryanto Yoso Wigroho, Daniel Krisna Murti. "High volume fly ash as substitution of fine aggregates with the proportion of 50%, 60%, and 70% to the shear strength of reinforced concrete beams", MATEC Web of Conferences, 2018
Publication | <1 % |
| 17 | Arya, Gaurav. "Models for recovering the energy landscape of conformational transitions from single-molecule pulling experiments", | <1 % |

18

Submitted to University of Abertay Dundee

Student Paper

<1 %

19

Hee-Chang Eun. "On the shear strength of reinforced concrete deep beam with web opening", The Structural Design of Tall and Special Buildings, 12/2006

Publication

<1 %

20

Vincenzo Colotti, Giuseppe Spadea. "An analytical model for crack control in reinforced concrete elements under combined forces", Cement and Concrete Composites, 2005

Publication

<1 %

21

Lee, J.-Y., K.-H. Kim, S.-W. Kim, and H. Choi. "Bond Strength Deterioration of Reinforced and Prestressed Concrete Members at Reversed Cyclic Loads", Strength of Materials, 2015.

Publication

<1 %

22

Xudong Qian, Yu Wang, J.Y. Richard Liew, Min-Hong Zhang. "A load-indentation formulation for cement composite filled pipe-in-pipe structures", Engineering Structures, 2015

Publication

<1 %

23

nora.nerc.ac.uk

Internet Source

<1 %

24

El-Sayed, Ahmed K.. "Shear capacity assessment of reinforced concrete beams with corroded stirrups", Construction and Building Materials, 2017.

Publication

<1%

Exclude quotes

Off

Exclude matches

< 8 words

Exclude bibliography

On